Collaborative Multimodal Drone-Based Remote Sensing for Levee Piping Detection

Tu Hu[1,†], Haoxiang Liu[1,†], Tongqi Wang[1], Shan Su[1], Changjun Chen[1*]

1School of Geodesy and Geomatics, Wuhan University, 129 Luoyu Road, Wuhan 430072, People's Republic of China;
hutu_whu@qq.com;liuhaoxiang@whu.edu.cn;wangtongqi@whu.edu.cn;sushan787426@163.com
* Correspondence: chencj@whu.edu.cn

Keywords: Levee Piping, Salient Object Detection, Image Overlap, Feature Analysis, Adaptive Thresholding.

Abstract

This paper proposes a collaborative multimodal unmanned aerial vehicle (UAV) remote sensing method for the early detection of levee piping in complex environments. Addressing the identification challenges caused by weak piping thermal anomaly signals and strong background interference, this method innovatively integrates infrared image saliency detection with multi-source information verification. First, by combining global and local saliency analysis, suspected low-temperature anomaly areas in the infrared image are enhanced and extracted. Subsequently, adaptive threshold segmentation is employed to achieve preliminary localization of suspicious areas. To suppress false alarms, the algorithm designs a multi-level filtering mechanism, sequentially screening candidate areas based on the physical characteristics and geographical priors of piping, such as minimum area, temperature distribution variance, and terrain conditions. Finally, point cloud intensity images are introduced for spatial overlap analysis, leveraging the complementary nature of infrared and LiDAR data for cross-validation, thereby achieving precise identification of piping areas. Experiments validated based on field data collected from multiple locations show that this method can effectively enhance the robustness and accuracy of piping detection in complex field environments, providing a reliable technical solution for intelligent levee inspection.

1. Introduction

Levee engineering is a critical component of flood control systems, and its safe operation is directly related to the safety of life and property along the coast. Under the conditions of high water levels during flood seasons, earth-rock dams are highly susceptible to hazards such as seepage and piping. If not detected and addressed in a timely manner, these hazards can easily trigger dam failure disasters. Therefore, achieving rapid, accurate, and non-contact detection of levee hazards is a key link in enhancing flood control and disaster reduction capabilities.

As one of the most destructive hazards for dams, the early-stage manifestations of piping are typically only local seepage and weak temperature anomalies. They often occur in complex environments with dense vegetation, undulating terrain, and uneven lighting, where targets are small in scale, irregular in shape, and have weak textural features, making them highly susceptible to being masked by background interference. Furthermore, limited by the principles of thermal infrared imaging, factors such as solar radiation, ground object reflection, and water vapor disturbance introduce a large number of false targets, further increasing detection difficulty. Therefore, accurately extracting weak thermal anomalies caused by piping within complex backgrounds and effectively suppressing environmental interference has become an urgent problem to be solved in current infrared inspection of levees.

Traditional levee inspection mainly relies on manual patrols, supplemented by point-based monitoring methods such as piezometers and pressure-measuring tubes. This approach is not only inefficient and limited in coverage but is also susceptible to weather, terrain, and personnel experience, making it difficult to meet the demands for high-frequency, large-scale inspections during flood seasons. In response to the limitations of traditional inspection methods, unmanned aerial vehicle (UAV) platforms equipped with high-precision thermal infrared and visible-light sensors have emerged. They can achieve non-contact, automated large-scale inspection of levees, quickly acquire temperature and image information of the dam surface, and significantly enhance[1] the early detection capability and inspection efficiency for concealed hazards like piping through real-time data transmission and processing.

In recent years, non-contact monitoring based on UAVs equipped with multiple sensors has yielded several achievements. (Zhou et al., 2022) achieved automatic identification of seepage in earth-rock dams by combining UAV passive infrared thermography with transfer learning based on AlexNet. (Li et al., 2023) achieved automatic identification of piping disasters in small and medium-sized river earth-rock dams by utilizing thermal infrared and visible-light images collected by UAVs, combined with an automatic identification algorithm based on temperature diffusion effect analysis. (Zhang et al., 2024) developed a dam seepage inspection system capable of automatically identifying seepage areas, based on a mobile robot platform, infrared image texture feature classification, and a deep transfer learning model. (Wang et al., 2024) achieved identification and localization of potential seepage areas in dams through a multi-level detection method, based on a UAV multi-sensor platform integrating thermal infrared cameras, RGB cameras, and LiDAR.

However, despite the potential shown by modern technologies like infrared thermography in detecting temperature anomalies related to water seepage, they still face significant challenges under complex field conditions. Specifically, these methods, when dealing with weak seepage signals in complex environments, are often affected by background clutter, terrain variations, and uneven illumination. This leads to issues such as high false alarm rates, insufficient sensitivity, and poor model generalization capability, making it difficult to achieve early identification and precise localization of hazards like piping.

Inspired by the saliency detection proposed by (Zhai et al., 2016) and the saliency filters by (Perazzi et al., 2012), this paper

† These authors contributed equally to this work.

https://doi.org/10.5194/isprs-archives-XLIX-B2-2026-1029-2026

proposes an automatic piping detection algorithm based on thermal infrared image saliency detection, adaptive threshold segmentation, and feature analysis. The method leverages the temperature anomalies caused by the difference in heat capacity between water and soil. It first uses an enhanced saliency detection model to extract low-temperature anomaly regions from thermal infrared images, combines this with point cloud intensity images for cross-validation using multi-source information, and performs analysis of patch overlap to suppress false alarms. Ultimately, it achieves high-precision identification of piping areas. This method possesses strong environmental adaptability and engineering portability, providing a new technological pathway for intelligent piping identification in complex levee environments.

2. Method

To achieve rapid discrimination of suspicious piping areas, this study constructed a set of algorithms based on saliency object detection and multi-layer recognition of piping features. This algorithm can quickly and effectively identify suspicious piping areas, providing favorable support for flood control, disaster mitigation, and levee inspection. Its overall process is divided into two steps, where the first step is to initially extract piping areas through infrared image saliency detection, and the second step is multi-layer discrimination based on piping features and multi-source data, with the framework of this algorithm shown in Figure 1.

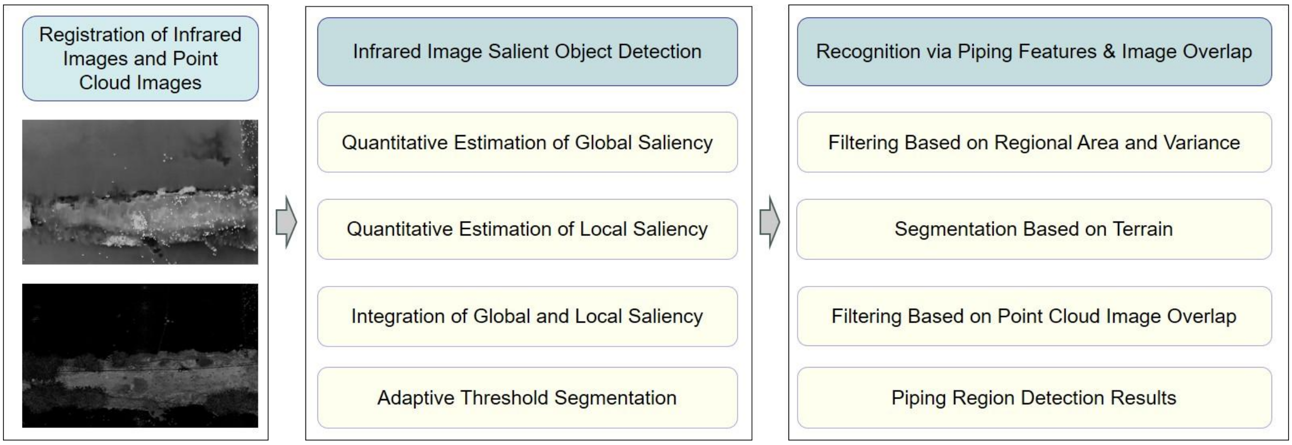

Figure 1. Workflow for infrared image salient object detection

2.1 Infrared image saliency detection

Dam piping is a primary form of seepage deformation failure, and its development process induces specific temperature field anomalies. Infrared thermography technology can non-contact acquire the surface temperature distribution, with its images intuitively reflecting the radiation differences of targets through different grayscale levels. Since piping seepage alters the thermal conduction properties of soil, leading to a significant temperature difference between the water exit point and the surrounding area, target detection using infrared images can effectively identify potential hazards in dams. This method offers the advantages of rapid and large-scale detection, enabling early localization and warning of piping, and providing crucial evidence for engineering safety assessment.

When performing dam target detection using infrared images, direct pixel-based analysis is susceptible to noise interference and relatively low computational efficiency. Therefore, this paper adopts the SLIC algorithm to perform superpixel segmentation on the image, aggregating pixels with similar features into more meaningful visual units. SLIC is an efficient superpixel generation method that performs local clustering based on color similarity and spatial proximity of pixels, capable of rapidly generating compact and uniform superpixel blocks. This method can significantly simplify the complexity of subsequent image processing, while better preserving the boundary structure of suspected seepage areas, providing a stable and reliable analytical foundation for subsequent target recognition.
Given that saliency analysis at a single scale struggle to comprehensively capture the anomalous features of piping areas within complex backgrounds, this paper will subsequently calculate image saliency from both global and local dimensions. Combining the two can achieve the goal of highlighting the most distinct targets from the background in the entire image while not missing weak temperature anomalies in local regions, thus balancing detection breadth and precision. Global saliency primarily evaluates the contrast between each pixel and the overall image features. It can quickly locate the most prominent suspected areas, providing a macro focus for analysis. Its role is to provide macro-level anomaly indication, avoiding missed detection of large-scale hazards. The calculation formula for global saliency is:

$$s_{\mathrm{global}}(r_i) = \sum_{j=1, j\neq i}^{N} w(r_j) D_r(r_i, r_j) \tag{1}$$

$$w(r_j) = \exp\left(1 - \frac{A(r_j) - \min\limits_{1\le i\le N}[A(r_i)]}{\max\limits_{1\le i\le N}[A(r_i)] - \min\limits_{1\le i\le N}[A(r_i)]}\right) \tag{2}$$

$$D_r(r_i, r_j) = \| c_i - c_j \| \tag{3}$$

where $w(r_j)$ = the weight parameter for region ri
$D_r(r_i, r_j)$ = gray distance between the two regions
$A(r_i)$ = the number of pixels in region ri
c_i = mean of region ri

Local saliency is calculated based on the contrast between a superpixel region and its neighboring areas, highlighting local anomalies through sliding windows or neighborhood analysis. For piping detection, local saliency can effectively identify isolated low-temperature targets, such as small-scale seepage points, enhancing detail perception capability and compensating for the shortcomings of global methods regarding subtle features. Its advantage lies in sensitivity to local thermal contrast, enabling rapid response to initial hazards. The calculation formula for local saliency is:

$$s_{\mathrm{local}}(r_i) = \sum_{r_j \in \Omega(r_i)} w(r_i, r_j) D_r(r_i, r_j) \quad (4)$$

$$w(r_i, r_j) = \exp\left(-\frac{d^2(r_i, r_j)}{\sigma}\right) \quad (5)$$

where $w(r_i,r_j)$ = the weight parameter between region r_i and r_j
$\Omega(r_i)$ = the set of neighbor regions of the region r_i
$d(r_i,r_j)$ = the Euclidean distance between the centers of region r_i and r_j
σ = image standard deviation

The method combining local and global saliency achieves complementary advantages. Local saliency captures detailed features, while global saliency provides overall context. Fusion by multiplication can simultaneously highlight high-contrast regions and suppress non-target interference. This combination strategy in piping detection can improve the signal-to-noise ratio, ensuring the completeness and accuracy of suspicious areas. The final saliency is obtained by multiplying the two, and its expression is:

$$s_{\mathrm{final}}(r_i) = s_{\mathrm{global}}(r_i) s_{\mathrm{local}}(r_i) \quad (6)$$

In levee piping detection, infrared images can capture temperature anomaly areas caused by piping. Due to the significant difference in specific heat capacity between the water in the piping area and the earthen dam (the specific heat capacity of water is approximately 4.2×10^3 J/(kg·°C), while that of soil is approximately 0.84×10^3 J/(kg·°C)), under solar radiation, localized temperature anomalies form at the piping outlet and its surrounding areas, manifesting as low-temperature or high-temperature regions in infrared images. However, infrared images are susceptible to environmental noise, illumination variations, and sensor errors, leading to uneven temperature distribution. To accurately segment piping areas, an adaptive threshold method is required. Based on the characteristic that piping temperature anomalies approximately follow a Gaussian distribution statistically, this paper constructs a Gaussian distribution probability density function (PDF) to fit the temperature histogram of the infrared image. By calculating the mean and standard deviation of the temperature data, a threshold is computed to segment the abnormal temperature regions from the background, achieving preliminary detection of piping areas. The formula for the Gaussian probability density function is as follows:

$$\mathrm{PDF}(i) = \frac{1}{\sigma\sqrt{2\pi}} e^{-\frac{(i-\mu)^2}{2\sigma^2}} \quad (7)$$

where σ = image standard deviation
μ = grayscale mean
PDF(i) = Gaussian probability density value for gray level i

2.2 Accurate piping identification fusing multi-source priors

In infrared images, piping areas exhibit localized temperature anomalies, but are susceptible to environmental interference that can generate false targets. Relying solely on single-modal data makes it difficult to ensure detection reliability. Therefore, the introduction of multi-modal remote sensing data for collaborative discrimination aims to enhance the robustness and accuracy of piping identification through complementary information. This method combines infrared and point cloud data, sequentially employing four strategies: removal of small connected regions, regional temperature variance filtering, regional terrain filtering, and point cloud intensity image overlap identification. These strategies comprehensively verify the physical characteristics of suspicious areas to suppress false detections and ensure the rationality of the detection results.

To improve the accuracy of piping detection, the operation of removing small connected regions is first implemented. In its early development stage, a piping hazard requires a minimum spatial scale to form seepage failure, while tiny regions in the image often originate from noise or irrelevant objects. By combining the ground resolution of images obtained from the UAV flight altitude, an adaptive threshold is set to filter out small connected regions, effectively eliminating these false targets.

Subsequently, leveraging the physical characteristic that temperature distribution within a piping area becomes uneven due to seepage water flow, the temperature variance of each remaining connected region is calculated. Since calm water surfaces or uniform soil backgrounds have low variance, while piping areas exhibit high variance, high-variance regions are retained to ensure the targets possess genuine thermal anomalies. Integrating the physical mechanism of piping with the statistical properties of infrared images can significantly enhance the algorithm's robustness against complex environmental interference.

Based on the geographical regularity that pipings frequently occur in low-lying areas, this algorithm adopts a terrain filtering strategy. This strategy uses elevation information derived from point cloud 3D coordinate data. By calculating the relationship between a connected region and its surrounding terrain, it determines whether the region belongs to a low-lying landform, thereby effectively excluding false targets in non-conforming locations such as high slopes or dam crests.

Furthermore, in point cloud intensity images, water surfaces appear as low-intensity hollows due to laser scattering, while piping areas exhibit anomalies in both infrared and point cloud modalities. By calculating the spatial overlap between the infrared saliency map and the point cloud intensity image, and quantifying the co-occurrence probability using the Intersection over Union, modality-specific noise such as shadows or metal components is effectively suppressed. This couples the complementary advantages of infrared sensitivity to low temperature and point cloud sensitivity to water bodies, thereby filtering out the regions that most conform to piping characteristics.

3. Result

This study utilizes the CHCNAV X500 quadrotor unmanned aerial vehicle (UAV) equipped with the AR10 multi-sensor data acquisition system, specifically designed for levee inspection, for experimental data collection. The system integrates an uncooled vanadium oxide (VOx) infrared camera (resolution: 640×512, pixel size: 12μm, NETD < 50mK), a 26-megapixel visible-light camera (pixel size: 3.76μm), and a laser scanner. The scanner operates at a wavelength of 1535nm, supports up to 8 returns, with a maximum pulse repetition rate of 300,000 points per

https://doi.org/10.5194/isprs-archives-XLIX-B2-2026-1029-2026

second, a scan line rate of 50-250 lines per second, and a ranging accuracy of 15mm @ 150m. It enables synchronous acquisition of GNSS/IMU, LiDAR, visible-light, and infrared data, with real-time transmission to a ground control station. Inspection flights are typically conducted at an altitude of 50-70 meters and a speed of 5-8 meters per second.

In China, the flood season typically begins in April each year. Accompanied by frequent heavy rainfall, river water levels rise rapidly, increasing the risk of hazards such as piping in levee engineering. To systematically study the identification mechanism of dam piping, this research utilized a UAV equipped with a multi-modal remote sensing detection system to conduct multiple batches of data collection in various locations, including Guangdong Province and Hubei Province. A total of 306 sets of thermal infrared images, LiDAR point cloud data, and visible-light image data were collected, all of which were precisely registered, and all these datasets contain piping areas.

3.1 Preliminary extraction of suspicious piping areas

Faced with the challenges of overall image blurriness and weak piping features in field levee scenarios, this study employed the SLIC superpixel segmentation and global-local saliency fusion algorithm to preprocess the original thermal infrared images. As shown in Figure 2, the selection of different superpixel parameters significantly impacts the results. Choosing appropriate parameters can not only improve detection efficiency but also greatly enhance detection accuracy.

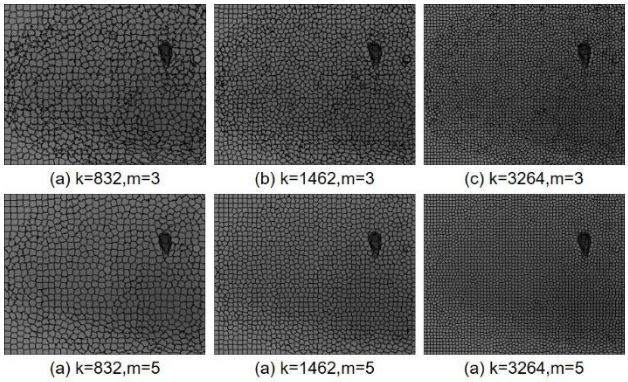

Figure 2. SLIC results under different parameters.

In superpixel segmentation, the parameter k controls the number of superpixels, directly affecting their size. A k value that is too small leads to excessively large superpixel sizes, which may obscure small piping targets; a k value that is too large increases computational load and introduces redundant details. The parameter m adjusts the compactness of superpixels, determining the degree of pixel aggregation. A value of m that is too high can cause segmentation to fail, while a value that is too low results in blurred boundaries, affecting regional consistency. This paper selects k=1462, corresponding to an initial size of approximately 15 pixels, ensuring precise segmentation of small targets while balancing algorithm efficiency. m is set to 3 to balance the ability to conform to the iregular boundaries of piping and the consistency of features within superpixels, thereby providing an optimized foundation for subsequent saliency detection.

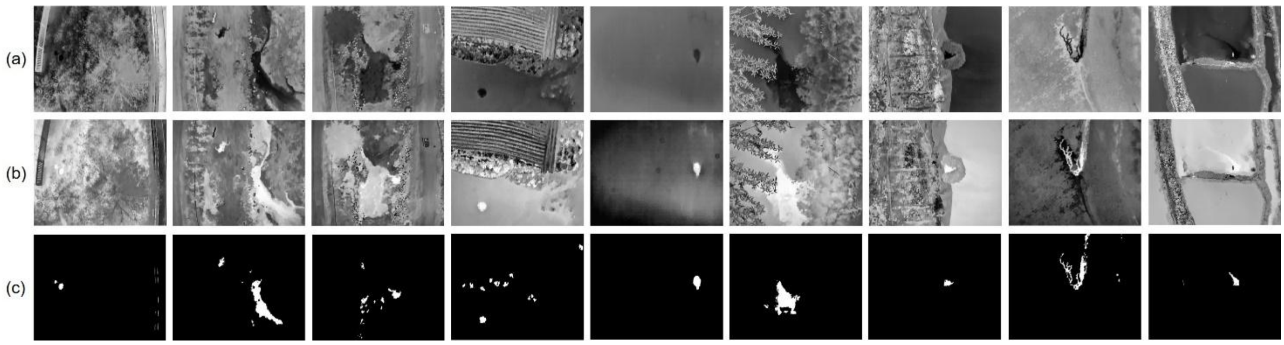

Figure 3. Salient object detection results. (a)Infrared image, (b)Saliency fusion image, (c)Adaptive threshold binary segmentation

As shown in Figure 3(b), in the image processed by global-local saliency fusion, the piping zone is effectively enhanced, appearing highlighted with clear edges and contours. On the basis of enhancing image contrast, the Gaussian probability density function (PDF) was constructed to fit the temperature histogram of the image. This adaptively determined the segmentation threshold, achieving automated preliminary extraction of suspicious areas. This method avoids the limitations of a fixed threshold and can adapt to temperature distribution variations under different environmental conditions.

Out of a total of 306 test datasets, this method successfully preliminarily extracted suspicious areas, including piping, from 294 datasets. The recall rate was 96.08%, and the missed detection rate was 3.92%. This result verifies the effectiveness of the saliency fusion and adaptive threshold strategy in capturing thermal anomaly signals of early-stage piping. Furthermore, the introduced SLIC superpixel segmentation resulted in more precise contours of the extracted areas, significantly reducing background pixel interference and providing superior target primitives for subsequent fine-grained discrimination based on multi-level features.

3.2 Piping Feature and Image Overlap Analysis

The initially extracted suspicious areas contain a large number of discrete, small-area connected regions and false targets that do not conform to piping characteristics. Therefore, at this stage, a series of filtering judgments based on multi-source prior knowledge is applied to progressively eliminate false detections and achieve precise localization.

As shown in Figure 4, the three-level feature filtering process designed in this study effectively eliminated false targets from the initially extracted suspicious areas. Firstly, based on the geoscientific prior knowledge that a piping requires a certain spatial scale, isolated tiny spots caused by image noise were filtered out using an adaptive area threshold. The result, shown in Figure 4(b), demonstrates that a large number of discrete, small connected regions were successfully removed.

Secondly, based on the physical characteristic that piping seepage leads to uneven temperature distribution, the temperature variance of each region was calculated. Regions with uniform temperature, such as calm water surfaces or homogeneous soil backgrounds, were filtered out. As shown in Figure 4(c), only genuine thermal anomaly regions exhibiting high variance characteristics were retained.

Next, by integrating elevation data provided by LiDAR point clouds, the topographic rationality of the remaining regions was verified, excluding responses from unreasonable locations such as high slopes or dam crests. The result, shown in Figure 4(d), indicates that the targets are concentrated in high-risk areas. After this sequential filtering, the algorithm correctly identified 283 piping regions from the 294 preliminary results. Among the total 306 test datasets, 283 instances of piping were ultimately detected, with 12 missed detections and 11 false detections, resulting in a recall rate of 92.48%. This lays a reliable foundation for subsequent precise localization based on image overlap analysis.

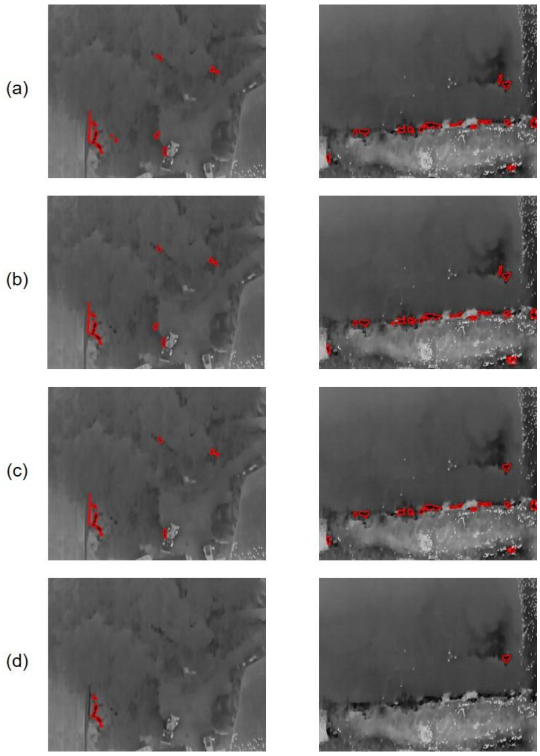

Figure 4. Results of physical feature discrimination. (a)Salient object detection results, (b)Small connected area filtering, (c)Temperature distribution filtering, (d)Terrain filtering.

After completing the three-level feature filtering based on area, temperature variance, and terrain, spatial overlap co-occurrence verification between infrared and point cloud intensity images is performed. In point cloud intensity images, the strong scattering effect of laser light on water surfaces leads to a sharp attenuation of the signal, resulting in extensive low-intensity or even zero-value void regions. By calculating the proportion of zero-value pixels in the entire point cloud image, the extent of open water surfaces in the inspection scene can be effectively assessed.
When a large water surface is present in the point cloud image, the void proportion is significant, and direct threshold segmentation loses discriminative power. Therefore, the algorithm instead uses the Otsu adaptive threshold to binarize the point cloud intensity image and performs spatial matching with each infrared suspicious region retained after the three-level filtering. For each candidate region, the proportion of its area occupied by zero-value pixels is calculated respectively in the original point cloud intensity image and its Otsu binarized result. A genuine piping water exit point, as a localized water body, should exhibit a dense zero-value response in at least one of the point cloud representations. Consequently, the algorithm retains those infrared candidate regions where the zero-value proportion exceeds 70% in the original point cloud image, or exceeds 80% in the Otsu binary image, thereby effectively coupling infrared thermal anomalies with point cloud water-body response features.

If the water surface area in the point cloud image is limited, resulting in a low proportion of zero-value voids, it indicates the absence of contiguous, large-area water body interference in the scene. In this case, the algorithm applies local saliency detection and Gaussian adaptive threshold segmentation similar to that used on the infrared image to the point cloud intensity image, obtaining all possible point cloud anomaly connected regions. Subsequently, the spatial Intersection over Union (IoU) between each candidate region retained via infrared multi-level filtering and all point cloud anomaly regions is calculated. A true piping point should trigger a significant response in both modalities simultaneously. Therefore, an infrared candidate region is finally confirmed as a reliable piping area only if its overlapping part with a point cloud anomaly region constitutes more than 20% of its own area and more than 50% of the point cloud anomaly region's area. The results of the final detection are shown in Figure 5.

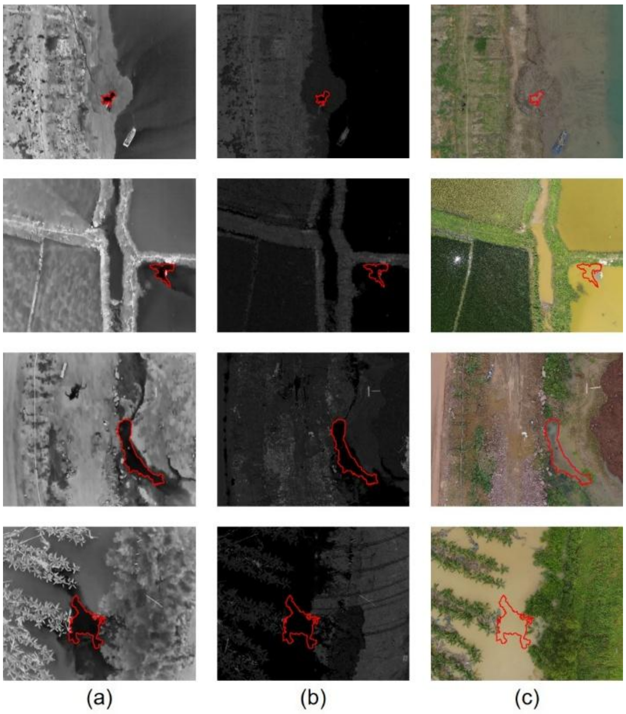

Figure 5. Comparison of piping detection results. (a)Infrared image, (b)Point cloud intensity image, (c)Visible light image.

After verification, the algorithm ultimately correctly detected 241 instances of piping areas from all 306 datasets. The algorithm's recall rate and precision rate reached 78.76% and 98.77%, respectively. This result verifies that the multi-level filtering and multi-modal co-occurrence strategy can effectively enhance the robustness and accuracy of piping identification in complex environments. This multi-modal cross-validation mechanism fully leverages the comparative advantages of infrared imaging's sensitivity to temperature and LiDAR's sensitivity to water bodies, ultimately achieving precise identification of piping areas and effective suppression of false alarms in complex environments.

4. Conclusions

This paper proposes a collaborative multimodal UAV remote sensing-based method for levee piping detection. The proposed saliency fusion and adaptive thresholding method effectively enhances the extraction capability for weak piping thermal anomaly signals in complex backgrounds. The designed multi-level, multimodal filtering and discrimination mechanism fully utilizes the physical characteristics and geographical priors of piping, significantly improving the robustness and engineering reliability of detection. Validated on a total of 306 field-collected datasets, this method ultimately achieved an overall correct detection rate of 78.76%, demonstrating its effectiveness and practicality in the early identification of levee piping in complex field environments. Future work will focus on incorporating data from more sensor modalities and exploring more efficient deep learning models to further enhance the generalization detection capability and real-time processing efficiency for piping hazards under different seasons, climatic conditions, and more complex terrain backgrounds.

References

Li, R., Wang, Z., Sun, H., Zhou, S., Liu, Y., & Liu, J., 2023. Automatic identification of earth rock embankment piping hazards in small and medium rivers based on UAV thermal infrared and visible images. *Remote Sensing*, 15(18), 4492.

Perazzi, F., Krähenbühl, P., Pritch, Y., & Hornung, A., 2012. Saliency filters: Contrast based filtering for salient region detection. *2012 IEEE Conference on Computer Vision and Pattern Recognition*, 733–740.

Wang, T., Su, S., & Chen, C., 2025. Dam leakage detection based on unmanned aerial vehicle multi-sensor. *ISPRS Annals of the Photogrammetry, Remote Sensing and Spatial Information Sciences*, 10, 161–166.

Zhai, L., Li, Y., & Su, Y., 2016. Inshore ship detection via saliency and context information in high-resolution SAR images. *IEEE Geoscience and Remote Sensing Letters*, 13(12), 1870–1874.

Zhang, S., 2024. *Design of Levee Leakage Inspection System Based on Infrared Image Processing*. M.S. thesis, Hefei University, Hefei, China.

Zhou, R., Wen, Z., & Su, H., 2022. Automatic recognition of earth-rock embankment leakage based on UAV passive infrared thermography and deep learning. *ISPRS Journal of Photogrammetry and Remote Sensing*, 191, 85–104.